Nanometal plasmons operating within quantum life-time: increasing the duration of the field trapped on the plasmonic solar cells

Mehmet Emre Taşgın
Department of Electrical & Electronics Engineering, Kırklareli University, 39020 Karahıdır, Kırklareli, Turkey and
Center for Advanced Researches, Kırklareli University, 39020 Karahıdır, Kırklareli, Turkey
(Dated: May 8, 2013)

We investigate the dynamics of the oscillations over a plasmonic nanometal when it is strongly coupled to a quantum dot (quantum emitter). We show that life time of the plasmonic oscillations can be increased several orders of magnitude, upto the decay time of the quantum emitter. Regarding the solar cell applications, such an effect gives rise to several orders of magnitude enhanced light-matter interaction. Because, i) incident sun light is trapped for a much longer time in the plasmonic nanometals which are doped over the surface of the solar cell and ii) life time of the slow light propagation lengthens. The new duration for plasmonic polarization is limited with the phase-coherence time of the sun light. Such an enhancement occurs due to the emergence of a phenomenon analogous to electromagnetically induced transparency (EIT). Additionally, we exhibit a complementary effect: the decay time of an electronically excited quantum emitter is severely shortened due to the antenna coupling.

PACS numbers:

I. INTRODUCTION

Ordinarily, the response of atoms to a electromagnetic field mimics a two-level quantum system since the degeneracy in the excited levels is masked out by dipole selection rules. However, if the dipole allowed excited state is microwave coupled to the forbidden one, the dielectric response will be severely modified [1]. A transparency window emerges at the resonance frequency, where without microwave drive an absorption peak would have been observed. This phenomenon is called as Electromagnetically Induced Transparency (EIT). The vanishing absorption is due to the following. The microwave coupling splits the dipole allowed excited state into two (Stark effect [2]). Since the splitting is smaller than the decay rate of the excited level, optical beam couples the ground state to each auxiliary levels. When the two Rabi oscillations are out of phase, absorption cancels and atom stays in the ground state [3–6]. The modified absorption is proportional to the decay rate of the dipole forbidden transition (much smaller) instead of the allowed one [1]. EIT-like schemes underlie in the physics of ultra-slow light propagation [7, 8] and index enhancement [9].

A similar phenomenon shown in Ref.s[4–6] takes place for the two coupled classical oscillators (C.O.), where the first one has a high damping rate (low-quality) and the second one has a low damping rate. When the low-quality C.O. is driven by a harmonic force, the absorbed power is governed with the damping rate of the high-quality one. Such a phenomenon takes place similarly due to the destructive interference of the two normal modes of the coupled oscillators system [4, 5]. In 2009, Soukoulis and colleagues demonstrated the classical analog of EIT in split ring resonators (SRRs) [10, 11]. They capacitively coupled a dipole SRR to a quadrupole one by closely placing the gaps of the two SRRs. Quadrupole SRR does not interact with the dipolar radiation, thus have higher quality factor when excited capacitively. Electromagnetic drive is on the dipolar oscillator, because incident radiation couples only to dipolar one. They showed that the response of the dipolar SRR exhibit a dip at the resonance frequency which is 43 THz.

Classical analog of EIT is shown to have many applications in the field of plasmonic physics. The coupling of dipole and quadrupole plasmonic modes of two rectangular thin plates (or rectangular gaps in metallic plates) manufactured in sub-micron dimensions are shown to exhibit EIT-like resonances and transparency windows [12–25]. In such devices, slow light propagation [26, 27], electromagnetically induced absorption [11, 20], and anomalous light transmission (where covering the subwavelength nanoaperture with gold nanodisk unexpectedly enhances the light transmission) [28] are observed. Former two effects are proposed to be used in solar cell applications[29, 30]. Because, they trap the light inside solar cell a longer time and provide enhanced light-matter interaction for pair creation [29]. The life time of the quadrupole moment limits the trapping time in solar cells.

Meanwhile, intense research is being conducted on the control of quantum objects (emitters) by coupling them to plasmonic excitations of nanoantennas [31]. The plasmon resonance frequencies of nanoantennas are in the range of a few hundred THz and they are tunable by changing the length/width and manufacturing material of the nanoantennas [32–38]. In 2010, van Hulst and colleagues coupled a quantum dot (QD) to a gold nanoantenna operating at 800nm [31]. They showed that QD (excited electronically) transfers the excitation energy [34] to the nano Uda antenna and radiates strongly directional. Plasmonic nanoparticles enhance the optical cross-section of a QD five orders of magnitude by localiz-

ing the incident light [39] This gives rise to potential for radiative communication between optical quantum emitters. It is shown that, such hybrid systems composed of coupled classical and quantum objects also display Fano resonances [39–48]. Absorption spectrum of the plasmonic nanoantenna displays a dip due to the destructive interference of the absorption paths. Similarly, presence of a nanometal near a quantum object modifies the emission futures of that quantum emitter. It is experimentally shown [49–51] that florescence of a QD can be enhanced to a factor of 8 by coupling it to a nanoantenna.

In this paper, we explore the dynamics of a classical oscillator (plasmonic oscillations on a nanometal) coupled to a quantum emitter (quantum dot [31, 32, 34, 49] or a nitrogen-vacancy center [35, 50, 51]). The plasmonic oscillations are driven by a harmonic force which stands for the incident sun light. The quantum emitter is placed on the nanoantenna (nanometal) to a position where dipolar plasmonic mode results very strong electric field localization (see Fig. 1). The localized electric field (five orders larger compared to the incident field [39]) interacts with the quantum emitter. Hence, a dipole-dipole type effective coupling occurs between the antenna and the quantum object [39–48]. Because of the coupling, a transparency window emerges at the center of the absorption spectrum of the antenna, see Fig. 2.

The damping rate of the plasmonic oscillation ($\gamma_q \sim 10^{12}$Hz) [11] is very large compared to the decay rate of the quantum object ($\gamma_{\rm eg} \sim 10^7$Hz). We show that, plasmonic oscillation evolves in time as if it has the tiny decay rate of the quantum emitter (see Fig. 6). Plasmonic oscillation reaches the steady state in a much longer ($\gamma_q/\gamma_{\rm eg}$) time. Such an observation has crucial importance in increasing the solar cell efficiency [29]. The common aim in the solar cell research is to increase the time that sun light spends in/on the semiconductor panels [26, 27, 29, 30, 53, 54]. The incident sun light is trapped in the silver/gold nanospheres (of diameter 80nm) which are placed on the surface of the solar cells by dewetting technique [29, 53, 54]. The trapped ($1/\gamma_q \sim 10^{-12}$ sec) and localized light interacts stronger with the semiconductor. This is much lower than the phase-coherence time of the sun light ($\tau \sim 10^{-8}$s), where in drive can be treated with a classical function $F(t) = Fe^{-i\omega t}$ [55, 56]. Thus, the new limit for the polarization duration is the phase-coherence time of the sun light. One can also increase the coherence time by using squeezed light [57, 58]. Hence, the nonlinear optical effects (e.g. second harmonic generation obtained in coupled nanowires [59]) can also be adopted to enhance the phase-coherence of the solar light.

In a coupled nanosphere-quantum emitter system trapping time lengthens to $1/\gamma_{\rm eg} \sim 10^{-7}$ sec, which corresponds to a several orders of magnitude increase in the pair formation efficiency for certain frequency ranges. Furthermore, absorption rate (plasmonic absorption) is reduced several orders of magnitude in the vicinity of the EIT window (see Fig. 3). Therefore, the slow-light [26, 27] can propagate for much more longer times which yields increased optical path.

We note that, in order to observe the duration enhancement for the plasmonic oscillation (polarization) one does not need a perfect matching between the plasmon resonance frequency and the quantum level spacing. In Fig. 6, we observe that position of the EIT center is determined by the quantum emitter. Self-assembled manufacturing of bio-molecules coupled to gold nanospheres is reported in Ref. [52]. Random distribution of such objects in solar cells would work as EIT-centers. Alternatively, sputtering of molecules on the de-wetted surface [53, 54] would work as well. The operation frequency would be determined by the molecular level spacing if its frequency is within the broad spectral width of the plasmon oscillation ($\omega_q \pm \gamma_q$). Using molecules with different quantum level spacing, EIT centers would operate for different frequencies. A variety of nanometals can be fit to a surface area of wavelength square.

We additionally observe that the decay time of the electronically excited quantum emitter to the ground state is also affected from the presence of the coupling. The excited quantum object decays to the ground state much faster than the natural decay rate $\gamma_{\rm eg}$, see Fig. 7.

The paper is organized as follows. In Sec. II A, we introduce the Hamiltonian for the coupled classical-quantum oscillator system. We drive the equations of motion for the system using density matrix formalism. We include the damping, quantum decay rates and the drive on the C.O.. In Sec. II B, we show the emergence of the EIT-like transparency window. At resonance, power absorption from the drive (by the C.O.) is governed by the quantum decay rate ($\gamma_{\rm eg}$) instead of C.O. damping (γ_q). In Sec. II C, we adopt an analytical form for the dipolar polarization in the plasmonic mode of the nanoantenna in the vicinity of the resonance. In Sec. II D, we picture the shift of the transparency window to the resonance of the quantum emitter ($\omega_{\rm eg}$), when classical and quantum oscillators are not perfectly tuned. In Sec. III, we show that the durations for reaching the steady-state is governed by the life-time of the quantum object ($1/\gamma_{\rm eg}$) for the coupled system. Thus, plasmons stay polarized for longer times even if the steady-state value for the polarization vanishes. In Sec. IV, we show that life time of the excited quantum emitter is shortened by the plasmon damping. In Sec. V, we summarize the paper and discuss the possible applications of the coupled classical-quantum system.

II. ANALOG OF EIT IN COUPLED CLASSICAL-QUANTUM OSCILLATORS SYSTEM

In this Section, we derive the equations of motion for a system where a classical oscillator (C.O.) is strongly coupled to a quantum emitter. The coupling is through dipole-dipole interaction and resonance frequencies of the

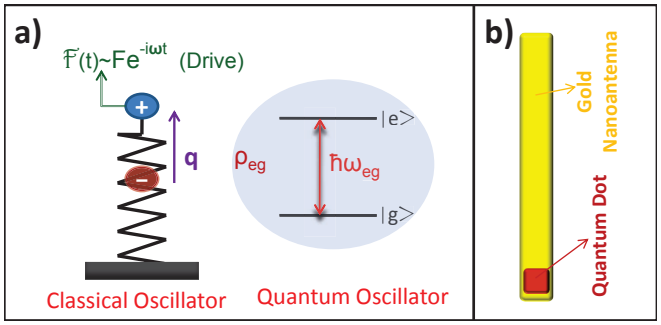

FIG. 1: (Color online) (a) A classical oscillator driven by an external harmonic source $F(t) = Fe^{-i\omega t}$ is coupled to a quantum oscillator of resonance frequency $\omega_{\rm eg}$. Interaction is dipole-dipole type: The dipole induced on the classical oscillator ($\sim q$) is coupled to the quantum one ($\sim \rho_{\rm eg}$). Quantum decay rate ($\gamma_{\rm eg}$) is very small compared to damping (γ_q). (b) The corresponding physical system for the model. A quantum dot is attached over the gold nanoantenna. Plasmonic oscillations on the antenna induces strong electric field at the ends of the bar. The localized electric field (10^5 times of the incident one [39]) couples to the quantum dot. The dipolar excitation of antenna is driven with the incident optical light.

oscillators are in the optical regime. We present the effective Hamiltonian for the system and derive the equations of motion using the commutation relations. We plot the power absorbed by the C.O. and depict the emergence of a transparency window (no absorption region) about the resonance frequency.

We consider a system where a quantum object (e.q. quantum dot, Nitrogen Vacancy center) is attached over a plasmonic nanoantenna that works in the classical regime [60] (see Fig. 1). The incident light couples to the plasmonic excitation mode of the nanoantenna. Coupling of light to single quantum emitter is of negligible strength compared to the plasmon. The dipole oscillations, which creates a very strong localized electric field over the nanoantenna, couples to the dipolar excitation of the quantum emitter. Quantum dot is placed at a position (end of the annoantenna) where dipolar plasmon mode gives the maximum electric field. Resultant interaction becomes dipole-dipole type. The effective system is: a quantum object coupled to a C.O. which is driven by an external source. The resonance of the plasmonic mode of the C.O. (ω_q) is tuned (by varying its size) close to the spacing between the ground and excited levels of the quantum oscillator ($\omega_{\rm eg}$).

A. Hamiltonian and Equations of Motion

The total hamiltonian ($\hat{H}$) for such a system can be written as the sum of the energy of the quantum object, energy of the plasmonic oscillations, and the dipole-dipole interactions energy

$$\hat{H}_0 = \hbar\omega_{\rm e}|{\rm e}\rangle\langle{\rm e}| + \hbar\omega_{\rm g}|{\rm g}\rangle\langle{\rm g}|\,, \tag{1}$$

$$\hat{H}_q = \frac{\hat{p}^2}{2m} + \frac{1}{2}m\omega_q^2\hat{q}^2\,, \tag{2}$$

$$\hat{H}_{\rm int} = \hbar g_c\hat{q}\left(e^{{\rm i}\theta}|e\rangle\langle g| + e^{-{\rm i}\theta}|g\rangle\langle e|\right)\,, \tag{3}$$

respectively. Dipole moment induced on the antenna (created by the plasmonic oscillations) is proportional to the displacement ($\hat{q}$) of the classical oscillator. The dipole moment of the quantum emitter is proportional to the off-diagonal matrix element $\rho_{\rm eg}$. In Eq. (3), $\hat{q}$ (oscillating with freq. ω_q) couples to the quantum dipole excitation $(e^{{\rm i}\theta}|e\rangle\langle g| + e^{-{\rm i}\theta}|g\rangle\langle e|)$, where g_c is in units of [freq./length] and $e^{{\rm i}\theta}$ is the phase of the matrix element. Parameter m is not directly referred in our derivations, it cancels similar to the case of quantization of Electromagnetic fields (see Chapter. 1 in Ref. [1]).

We use the commutation relations (e.g. $i\hbar\dot{\hat{q}} = [\hat{q}, \hat{H}]$) in deriving the equations of motion (EM). We keep $\hat{q}$ quantum up to a step in order to avoid any fault in the EM. After obtaining the dynamics in the quantum approach, we carry $\hat{q}$ to classical ($q(t)$). Using the rotating wave approximation (RWA), equations take the form

$$\ddot{q}_0(t) + \gamma_q\dot{q}_0(t) + \omega_q^2 q_0(t) + \frac{\hbar}{m}g_c e^{-{\rm i}\theta}\rho^*_{\rm eg}(t) = \frac{F}{m}e^{-{\rm i}\omega t}\,, \tag{4}$$

$$\dot{\rho}_{\rm eg}(t) = ({\rm i}\omega_{\rm eg} - \gamma_{\rm eg})\rho_{\rm eg} - {\rm i}g_c e^{-{\rm i}\theta}q_0^*(\rho_{\rm ee} - \rho_{\rm gg})\,, \tag{5}$$

$$\dot{\rho}_{\rm ee}(t) = -\gamma_{\rm e}\rho_{\rm ee}(t) - {\rm i}g_c\left(e^{{\rm i}\theta}q_0\rho_{\rm eg} - {\rm c.c.}\right)\,, \tag{6}$$

where we use the complex amplitude $q_0(t) \sim e^{-{\rm i}\omega t}$ for describing oscillations. It is related to the displacement of the C.O. as $q(t) = q_0(t) + q_0^*(t)$. In Eq. (4), we introduce the harmonic driving force $\left(\frac{F}{m}e^{-{\rm i}\omega t}\right)$, of frequency ω, on the plasmonic oscillator. Density matrix elements $\rho_{\rm ee}$, $\rho_{\rm gg}$, and $\rho_{\rm eg}$ belongs to the quantum emitter. $\gamma_{\rm ee}$ is the decay rate of the quantum emitter from the excited state to the ground state. Decay rate of the off-diagonal matrix element $\rho_{\rm eg}$ (or the polarization of the quantum emitter) is represented by $\gamma_{\rm eg} = \gamma_{\rm ee}/2$. The damping rate of the classical (plasmonic) oscillator is γ_q. Since $\gamma_{\rm ee}$ belongs to a quantum object, we have $\gamma_{\rm ee} \gg \gamma_q$. In example, the typical value for the decay rate of a molecular excitation is $\gamma_{\rm ee} \simeq 10^7$Hz, whereas the damping rate of plasmonic oscillation is $\gamma_q \simeq 10^{12}$Hz [11]. The constraint on the conservation probability $\rho_{\rm ee} + \rho_{\rm gg} = 1$ accompanies Eq.s (4-6).

We seek solutions of the form [4, 5]

$$q_0(t) = \tilde{q}_0 e^{-i\omega t} \quad \text{and} \quad \rho_{\rm eg}(t) = \tilde{\rho}_{\rm eg}e^{-{\rm i}\omega t}\,, \tag{7}$$

for the long term (steady-state) behaviour, where $\tilde{q}_0$ is complex number and related to the displacement of the C.O. as

$$q(t) = \tilde{q}_0 e^{-i\omega t} + \tilde{q}_0 e^{i\omega t}. \tag{8}$$

Density matrix element (of amplitude $\tilde{\rho}_{\rm eg}$) oscillates with the source frequency in the steady state. Inserting Eq.

(7) into Eq.s (4-6), we obtain the equations

$$(\omega_q^2 - \omega^2 - \mathrm{i}\gamma_g\omega)\bar{q} + f_c\omega_q e^{-\mathrm{i}\theta}\tilde{\rho}_{\mathrm{eg}}^* = \bar{F}\ , \quad (9)$$

$$[\mathrm{i}(\omega - \omega_{\mathrm{eg}}) + \gamma_{\mathrm{eg}}]\,\tilde{\rho}_{\mathrm{eg}} + if_c e^{-\mathrm{i}\theta}\bar{q}^*(\rho_{\mathrm{ee}} - \rho_{\mathrm{gg}}) = 0\ , \quad (10)$$

$$\gamma_{\mathrm{ee}}\rho_{\mathrm{ee}} = -if_c\left(e^{i\theta}\bar{q}\tilde{\rho}_{\mathrm{eg}} - e^{-i\theta}\bar{q}^*\tilde{\rho}_{\mathrm{eg}}^*\right)\ , \quad (11)$$

relating the solutions for the slowly varying variables $\bar{q}$, $\tilde{\rho}_{\mathrm{eg}}$ and populations ρ_{ee} and ρ_{gg}. We have the additional equation $\rho_{\mathrm{ee}} + \rho_{\mathrm{gg}} = 1$ for the number (probability) conservation. $\bar{q} = \tilde{q}/a_0$ is the dimensionless (scaled) slowly varying (complex) displacement of the C.O., with $a_0 = (\hbar/m\omega_q)^{1/2}$ is the characteristic oscillator length. $f_c = g_c a_0$ is the coupling frequency (strength) and $\bar{F} = F/ma_0$ is the scaled force, in units of $[\mathrm{freq.}]^2$. We note that, in Eq. (10), scaling results $\frac{\hbar}{m}\frac{g_c}{a_0} = \frac{\hbar}{m}\frac{g_c a_0}{a_0^2} = g_c\omega_q$. Therefore, we do not refer to mass m any more.

B. Transparency Window in Absorption Spectra

We solve the set of nonlinear equations (9-11) and we obtain the response of the coupled classical-quantum oscillators system to a driving harmonic field (force). In the solutions, we make the assumption that driving force ($\bar{F}e^{-i\omega t}$) has always been on (till $t = -\infty$), implicitly.

Regarding the plasmonic oscillations, $q(t) = \tilde{q}_0 e^{-i\omega t} + \tilde{q}_0 e^{i\omega t}$ corresponds to dipolar polarization on the antenna. Thus, real/imaginary part of $\tilde{q}_0$ refers to the polarization/absorption. This is analogues to the relation $\mathbf{P}_\omega = \chi(\omega)\mathbf{E}_\omega$, where $\mathbf{P}$, $\mathbf{E}$, and χ stand for Polarization, Electric field, and dielectric susceptibility, respectively. An equivalent relation can be calculated also from the power that force does on the oscillator (force×velocity) [4, 5] per cycle,

$$P(t) = \mathrm{Re}\left\{-i\omega F\tilde{q}\right\} = \mathrm{Im}\left\{\omega F\tilde{q}\right\}\ . \quad (12)$$

Therefore, absorbed power is proportional to the imaginary part of the $\tilde{q}$, as discussed above. In Fig. 2, we plot the absorbed power for varying drive (source) frequency ω. We take the resonance frequency of the plasmonic mode equal to the quantum level spacing, i.e. $\omega_{\mathrm{eg}} = \omega_q$. When the C.O. is not coupled with the quantum object, absorption shows a peak at the resonance $\omega = \omega_q$ (dashed-line in Fig. 2). On the other hand, if the C.O. is coupled to the Q.O. with coupling strength $f_c = 0.1\omega_q$, emergence of a transparency window at the center of the absorption peak ($\omega = \omega_q$) is observed (solid-line in Fig. 2). In the vicinity of $\omega = \omega_q$, the absorbance is proportional to the quantum decay rate γ_{eg} instead of the classical one γ_{q} similar to Ref.s [1, 4, 5] (see Eq. (18) below).

Regarding plasmonic oscillations, $q(t)$ corresponds to polarization field in the antenna. So, In Fig. 3, we plot the nanoantenna polarization $\mathrm{Re}\{\bar{q}\}$ (solid-line) together with the antenna absorption ($\mathrm{Im}\{\bar{q}\}$). Fig. 3 depicts the common form of the EIT-like response [1].

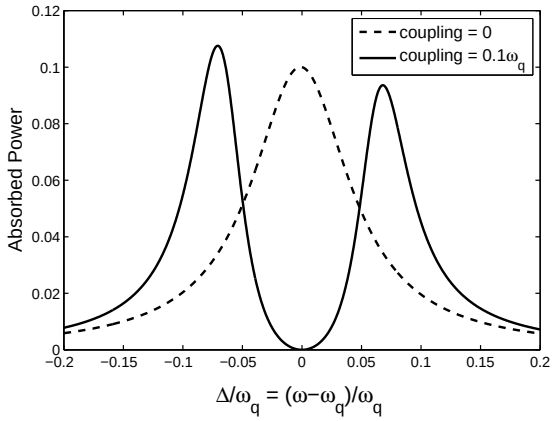

FIG. 2: The power classical oscillator (nanoantenna) absorbs from the driving force (electromagnetic field). When the nanoantenna operates alone, absorption is peaked (dashed-line) about the resonance frequency frequency of the antenna (ω_q). If the nanoantenna is coupled to a quantum oscillator (e.g. quantum dot), a transparency window occurs (solid-line) in the mid of the absorption peak. The new absorption at resonance is determined by the decay rate of the quantum dot ($\gamma_{\mathrm{eg}} \simeq$10MHz), which is several orders of magnitude smaller compared to the damping ($\gamma_q \simeq$THz). The quantum level spacing is perfectly tuned with the resonance of antenna, e.g. $\omega_{\mathrm{eg}} = \omega_q$. The damping and quantum decay rates $\gamma_q = 0.1\omega_q$ and $\gamma_{\mathrm{eg}} = 0.5 \times 10^{-4}\omega_q$ are used in the simulation. Driving force is $\bar{F} = 0.01$.

Fig. 4 plots the corresponding values for the polarization in the quantum dot ($\tilde{\rho}_{\mathrm{eg}}(\omega)$) and the excitation fraction ($\rho_{\mathrm{ee}}(\omega)$). We see that (solid-line in Fig. 4b), quantum dot stays polarized ($\mathrm{Re}\{\rho_{\mathrm{eg}}\} \neq 0$) without absorption ($\mathrm{Im}\{\rho_{\mathrm{eg}}\} = 0$) at resonant drive $\omega = \omega_q$. In addition, quantum dot becomes partially excited ($\rho_{\mathrm{ee}} \neq 0$) about the resonance. The reason for the asymmetric absorption peaks in Fig. 2 is due to the antisymmetric absorption profile (about $\Delta = 0$) of the quantum oscillator. For $\omega > \omega_q$, quantum object display gain ($\mathrm{Im}\{\rho_{\mathrm{eg}}\} < 0$) in the coupled system. Such asymmetric absorption (scattering) profiles are common to Fano resonances [23].

C. Analytical form for antenna polarization ($\bar{q}$)

Exact expressions for $\bar{q}$ are cumbersome since they include the solutions of the cubic equations. However, analytical expressions where the solution for the population inversion $y = \rho_{\mathrm{ee}} - \rho_{\mathrm{gg}}$ left implicit give us clues about the response of the coupled system. When the expression for ρ_{eg}, obtained from Eq. (9), is used in Eq. (10), one obtains

$$\bar{q} = \bar{F}\frac{(\omega - \omega_{\mathrm{eg}}) + i\gamma_{\mathrm{eg}}}{D_{\mathrm{R}} + iD_{\mathrm{I}}}\ , \quad (13)$$

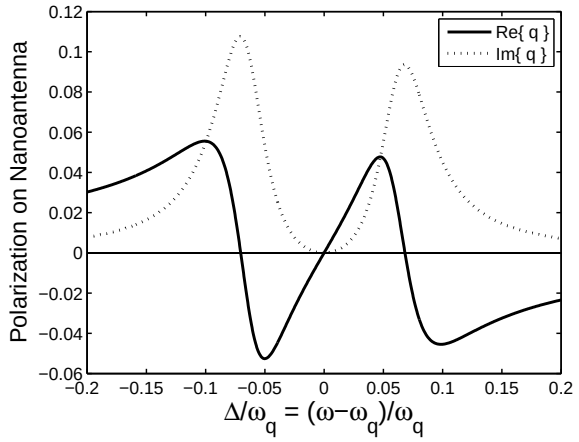

FIG. 3: The real (solid-line) and the imaginary (dotted-line) parts of the displacement ($\bar{q}$) of the classical oscillator. Real part gives the polarization induced on the nanoantenna. Imaginary part is proportional to the antenna absorption. We clearly observe the EIT-like behaviour [1, 4, 5, 10, 11]. The parameters are the same with Fig. 2.

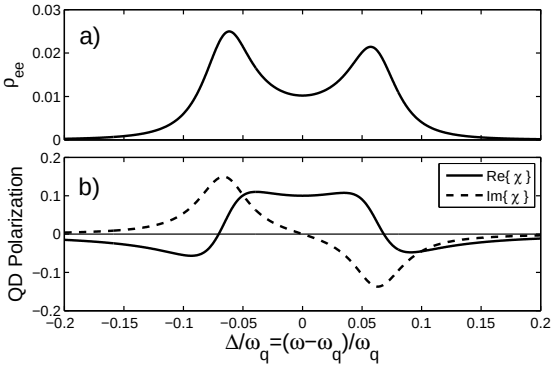

FIG. 4: The corresponding steady state values for the (a) excitation fraction and (b) polarization in the quantum dot, which is coupled to the nanoantenna (classical oscillator). At resonance, quantum dot stays polarized ($\mathrm{Re}\{\rho_{\mathrm{eg}}\} \neq 0$) with a finite excitation probability ($\rho_{\mathrm{ee}} \neq 0$). The absorption of the quantum dot vanishes at resonance ($\mathrm{Im}\{\rho_{\mathrm{eg}}\} = 0$).

where

$$D_{\mathrm{R}} = (\omega - \omega_{\mathrm{eg}})(\omega_q^2 - \omega^2) + \gamma_q \gamma_{\mathrm{eg}} \omega - f_c^2 \omega_q y \qquad (14)$$

$$D_{\mathrm{I}} = \gamma_{\mathrm{eg}}(\omega_q^2 - \omega^2) - \gamma_q \omega(\omega - \omega_{\mathrm{eg}}) \qquad (15)$$

are the real and imaginary parts of the denominator in Eq. (13). $\bar{F}$ is the scaled force in units of $[\mathrm{freq.}]^2$. The value of population inversion y is determined by solving the cubic equation

$$\frac{1+y}{2} = -\frac{f_c^2 y}{(\omega - \omega_{\mathrm{eg}}) + \gamma_{\mathrm{eg}}^2} |\bar{q}|^2 \,, \qquad (16)$$

which is obtained by using the expression for ρ_{eg} in Eq. (11). From Eq. (16) it can be seen that $y < 0$ must be satisfied. Among the three roots for y, only one is real or satisfies all of the equation (9-11) [61].

When $\underline{\omega = \omega_q = \omega_{\mathrm{eg}}}$, Eq. (13) simplifies to

$$\bar{q} = i \frac{\bar{F} \gamma_{\mathrm{eg}}}{(\gamma_q \gamma_{\mathrm{eg}} - f_c^2 y)\, \omega_q} \,, \qquad (17)$$

that is purely imaginary and resulting no polarization. Since γ_{eg} is very small compared to all frequencies, absorption is represented by

$$P \simeq \bar{F} \gamma_{\mathrm{eg}} / (-f_c^2 y) \qquad (18)$$

which is proportional to γ_{eg}, not γ_q [4, 5]. For $\omega = \omega_q = \omega_{\mathrm{eg}}$ and $\gamma_{\mathrm{eg}} \to 0$, the equation for y [that is Eq. (16)] simplifies to

$$y^2 + y + c = 0 \,, \qquad (19)$$

where $c = 2\bar{F}^2 / f_c^2 \omega_q^2$. Eq.(19) has real solutions only if discriminant is nonnegative, that is if $\bar{F} < \left(f_c \omega_q / 2\sqrt{2}\right)$. Hence, in the linear regime (when drive is small) y has the real solutions

$$y_{1,2} \simeq -\frac{1}{2} \pm \frac{(1-4c)^{1/2}}{2} \,. \qquad (20)$$

D. Shift of Trancparency Window when C.O. is not perfectly tuned to Q.O. ($\omega_{\mathrm{eg}} \neq \omega_{\mathrm{q}}$)

When the resonance frequency of the dipole mode of the plasmonic excitation of the nanoantenna does not match the quantum level separation (ω_{eg}), the bahavior of the EIT-like response is modified. The position, where EIT occurs shifts to $\omega \simeq \omega_{\mathrm{eg}}$ (see Fig. 5). This takes place due to the following effect. The spectral width of the quantum oscillator (quantum dot) $\Delta_{\mathrm{qua}} \simeq \gamma_{\mathrm{eg}} = 0.001\omega_q$ is very tight compared to the spectral width of the C.O. $\Delta_{\mathrm{cls}} = 0.1\gamma_q$. Thus, in order to establish the coupling, C.O. rearranges its frequency (within $\Delta_q \sim \gamma_q$) in order to match the energy spacing of the quantum system.

III. ENHACED DURATION FOR PLASMONIC OSCILLATIONS

In Fig. 6, we plot time evolutions of the antenna polarization ($\bar{q} = \mathrm{Re}\{\bar{q}\} + i\mathrm{Im}\{\bar{q}\}$) when there is no coupling (Fig. 6a) between the classical-quantum oscillators and in the existence of coupling $f_c = 0.1\omega_q$ (Fig. 6b). Quantum level separation is $\omega_{\mathrm{eg}} = 1.01\omega_q$, decay rates are $\gamma_q = 0.1\omega_q$ and $\gamma_{\mathrm{eg}} = 0.0005\omega_q$. We observe that coupled oscillator reaches the steady state in the order of $\gamma_q/\gamma_{\mathrm{eg}} \sim 200$ times longer compared to the uncoupled one. Thus, the coupled system remains polarized for a much longer time even if finally it reaches zero polarization state (not zero in Fig. 6b). In the physics of solar cells, this corresponds to 200 times increase in the probability of pair formation, when the radiation is trapped in

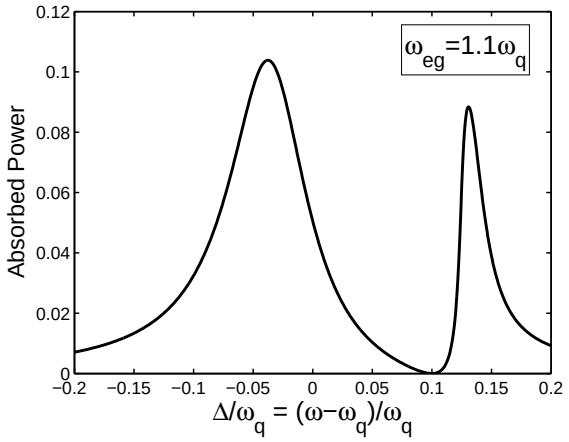

FIG. 5: The spectral variation of the absorbed power on the nanoantenna when the resonance frequency of the antenna (ω_q) is not perfectly tuned to the quantum level spacing ($\omega_{\rm eg}$). The position, where EIT-like response occurs, shifts to the quantum resonance $\omega = \omega_{\rm eg} = 1.1\omega_q$. Antenna can rearrange its operation frequency with in its spectral width $\pm\gamma_q = \pm 0.1\omega_q$ in order to match the quantum oscillation. The coupling strength is $f_c = 0.1\omega_q$ and driving force is $\bar{F} = 0.01$.

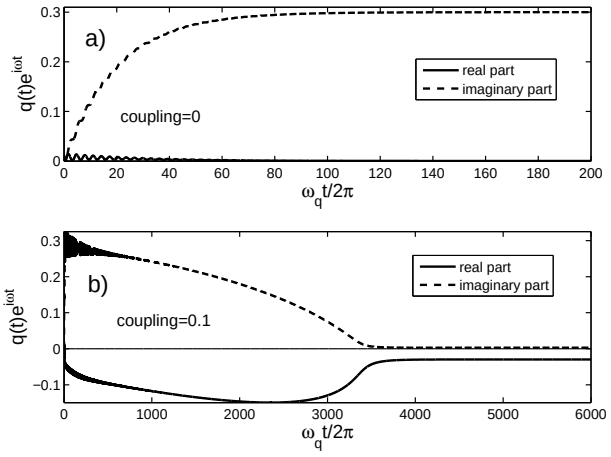

FIG. 6: Comparison of the durations for the two system to reach the steady-state polarization. Only the C.O. is driven by the harmonic force. a) Nanoantenna (C.O.) is not coupled to the quantum dot. Antenna polarization (Re$\{q\}$) reaches the steady-state at about $\omega_q t = 2\pi \times 200$. b) Nanoantenna is coupled to the quantum dot with coupling strength $f_c = 0.1\omega_q$. Antenna reaches the steady-state in about $\omega_q t = 2\pi \times 4000$. Coupled nanoantenna stay polarized for about $\gamma_q/\gamma_{\rm eg} \simeq 200$ times longer compared to the uncoupled one. Regarding solar cells, this corresponds enhanced light-matter interaction [29, 30, 53, 54]. Quantum level spacing is $\omega_{\rm eg} = 1.01\omega_q$. Decay rates are $\gamma_q = 0.1\omega_q$ and $\gamma_{\rm eg} = 0.0005\omega_q$. Driving force is $\bar{F} = 0.03$. We note that coherent drive time is limited with the phase-coherence of the sun light($\tau \sim 10^{-8}$s) of the sun light in solar cell applications [55, 56].

the localized electric field of the plasmon excitation. On the other hand, we note that the duration of the steady state (or period of the polarization duration) is limited with the coherence time of the sun light ($\tau \simeq 10^{-8}$s) in solar cell applications.

A similar effect occurs when a dipolar plasmon mode is coupled to a high-life quadrupole plasmon mode: full classical analog of EIT [29, 30, 53, 54]. However, the life time for a quantum excitation is much longer than the classical quadrupole plasmon one.

IV. MODIFIED DECAY TIME FOR QUANTUM EMITTER

Next, we focus on the dynamics of the quantum emitter. In Fig. 7, the quantum dot is prepared initially in the excited state ($\rho_{\rm ee} = 1$). There exists no drive, but quantum dot is coupled with a strength of $f_c = 0.1\omega_q$ to the nanoantenna. Comparing Fig. 7a and Fig. 7b, the coupled composite system emits the energy in a much shorter time (about 200 times).

Such an effect has already been observed [49–51]: fluorescence of a quantum emitter is enhanced when a nanometal is placed close to it. The enhancement is attributed to the change in the density of states due to the hybridization of the quantum dot and the nanometal [51]. Here, we observe a parallel effect due to the following. The effective decay rate of the quantum emitter is strongly modified by the damping rate of the plasmonic antenna.

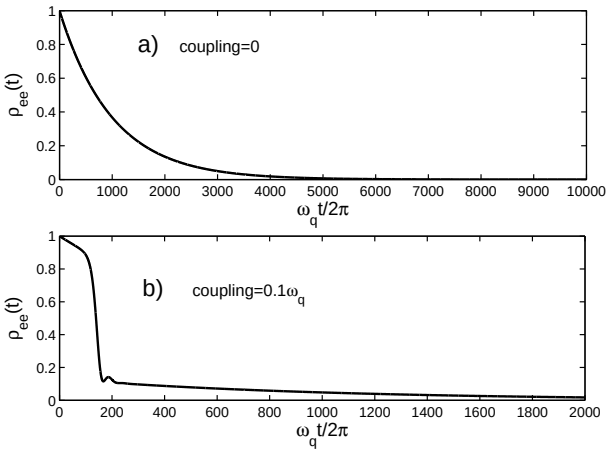

FIG. 7: Comparison of the durations for the excited quantum emitter to decay into the ground state. Quantum emitter is prepared initially in the excited state ($\rho_{\rm ee} = 1$) and there is no applied drive. a) Quantum dot is not coupled to nanometal. Decay to ground state happens in natural decay time $1/\gamma_{\rm eg} \sim 2000$. b) Quantum dot is coupled to nanometal with strength $f_c = 0.1\omega_q$. The decay of the composite system takes only ~ 200 time. Quantum level spacing is $\omega_{\rm eg} = 1.01\omega_q$. Decay rates are $\gamma_q = 0.1\omega_q$ and $\gamma_{\rm eg} = 0.0005\omega_q$. Driving force is $\bar{F} = 0.03$.

V. SUMMARY AND CONCLUSIONS

Incident sun light couples very strongly to the nanometal plasmons placed in solar cells. Trapped intense radiation results enhanced light-matters interaction [29]. However, this oscillations last in only about $1/\gamma_q \sim 10^{-12}s$ and light is re-radiated in different frequencies (heat). We show that the life-time of the light trapping in plasmonic oscillations can be increased upto the quantum decay time $1/\gamma_{\rm eg} \sim 10^{-7}$s. The dynamics of the driven plasmons is governed by the life time of the quantum emitter (see Fig. 6) which is coupled to it. The new life time is limited with the coherence time of the driving source [55, 56].

The presence of such an effect is due to the semiquantum–semiclassical analog of electromagnetically induced transparency (EIT) [1]. The coupling of the quantum object creates an additional oscillation mode whose frequency is within the uncertainty window (proportional to the damping rate) of the classical oscillator. The two normal modes of the classical oscillator interfere destructively and absorption cancels. A transparency window emerges at the center of the absorption peak of the plasmonic nanometal. A similar version of duration enhancement also occurs in the full-classical analog of EIT [4, 5, 10], where a dipole mode is coupled to a high-life quadrupole mode [11, 53, 54]. However, the life time of quantum excitation is highly large compared to the quadrupole mode plasmon life time.

Life-time enhancement can be utilized in photovoltaics to improve pair creation efficiency [29]. The metallic nanoparticles (diameter ∼80nm) –placed with dewetting technique [54]– can be combined with desired quantum emitters by sputtering the molecules. Since the position of the EIT window is determined by the frequency of the quantum level spacing (see Fig. 6), operation frequencies can be tuned with molecules. Several number of such nanometal–molecule combination can fit to a wavelength square. Hence, molecules of different frequency spacings can be used at once. We note that effective bandwidth of duration enhancement (of EIT window) is crudely about $\pm\gamma_q/4$ around the transparency window, see Fig. 2.

Moreover, the slow light propagation occurring within the transparency window last much longer. Regarding the macroscopic light propagation inside the solar cell, this effect additionally increases the optical path length.

On the other hand, pronounced phenomenon of duration enhancement cannot be applied to the case of direct coupling between plasmonic nanometals and QD solar cells [63]. This is because, plasmonic coupling also possible to increase the pair recombination rate (see Fig. 7) in QD solar cells.

Acknowledgments

I acknowledge support from TÜBİTAK-KARİYER Grant No. 112T927 and TÜBİTAK-1001 Grant No. 110T876. I specially thank Gürsoy B. Akgüç for guiding discussions and his intensive help with the manuscript. I specially thank T. Çetin Akıncı and Serhat Şeker for their motivational support.

[1] Chapter 7 in M.O. Scully and M.S. Zubairy, *Quantum Optics* (Cambridge University Press, Cambridge, U.K., 1997).
[2] W. Voigt, Annalen der Physik, **4**, 197 (1901).
[3] S.E. Harris and J.J. Macklin, Phys. Rev. A **40**, 4135 (1989).
[4] C.L.G. Alzar, M.A.G. Martinez, and P. Nussenzveig, Am. J. Phys. **70**, 37 (2002).
[5] C.L.G. Alzar, M.A.G. Martinez, and P. Nussenzveig, arXiv:quant-ph/0107061v1 (2001).
[6] A.G. Litvak and M.D. Tokman, Phys. Rev. Lett. **88**, 095003 (2002).
[7] T.F. Krauss, Nature Photonics **2**, 448 (2008).
[8] M.F. Yanik and S. Fan, Phys. Rev. Lett. **92**, 083901 (2004).
[9] M. Fleischhauer, C.H. Keitel, M.O. Scully, C. Su, T. Ulrich, and S.-Y. Zhu, Phys. Rev A **46**, 1468 (1992).
[10] P. Tassin, Lei Zhang, Th. Koschny, E.N. Economou, and C.M. Soukoulis, Phys. Rev. Lett. **102**, 053901 (2009).
[11] P. Tassin, Lei Zhang, R. Zhao, A. Jain, Th. Koschny, and C.M. Soukoulis, Phys. Rev. Lett. **109**, 187401 (2012).
[12] N. Liu, L. Langguth, T.Weiss, J. Kästel, M. Fleischhauer, T. Pfau, and H. Giessen, Nature Mat. **8**, 758 (2009).
[13] X. Liu, J. Gu, R. Singh, Y. Ma, J. Zhu, Z. Tian, M. He, J. Han, and W. Zhang, Apl. Phys. Lett. **100**, 131101 (2012).
[14] B. Lukyanchuk, N.I. Zheludev, S.A. Maier, N.J. Halas, P. Nordlander, H. Giessen, and C.T. Chong, Nature Mat. **9**, 707 (2010).
[15] R.D. Kekatpure, E.S. Barnard, W. Cai, and M.L. Brongersma, PRL **104**, 243902 (2010).
[16] A. Artar, A.A. Yanik, and H. Altug, Nano Lett. **11** 1685 (2011).
[17] A.E. Çetin, A. Artar, M. Turkmen, A.A. Yanik, and H. Altug, Opt. Express **19**, 22607 (2011).
[18] Z. Ye, S. Zhang, Y. Wang, Y.-S. Park, T. Zentgraf, G. Bartal, X. Yin, and X. Zhang, Phys. Rev. B **86**, 155148 (2012).
[19] N. Liu, T Weiss, M. Mesch, L. Langguth, U. Eigenthaler, M. Hirscher, C. Sönnichsen, and H. Giessen, Nano Lett. **10**, 1103 (2010).
[20] R. Taubert, M. Hentschel, J. Kaästel, and H. Giessen, Nano Lett. **12**, 1367 (2012).
[21] N. Papasimakis, V.A. Fedotov, N.I. Zheludev, and S.L. Prosvirnin, Phys. Rev. Lett. **101**, 253903 (2008).
[22] J. Chen, Z. Li, S. Yue, J. Xiao, and Q. Gong, Nano Lett. **12** 2494 (2012).
[23] A.E. Miroshnichenko, S. Flach, and Y.S. Kivshar, Rev. of Mod. Phys. **82**, 2257 (2010).
[24] S. Longhi, Phys. Rev. A **79**, 023811 (2009).

[25] C. Zheng, X. Jiang, S. Hua, L. Chang, G. Li, H. Fan, and M. Xiao, Opt. Express **20**, 18319 (2012).

[26] Y. Huang, C. Min, and G. Verosnis, Appl. Phys. Lett. **99**, 143117 (2011).

[27] C. Wu, A.B.Khanikaev, and G. Shvets, Phys. Rev. Lett. **106**, 107403 (2011).

[28] K. Imura, K. Ueno, H. Misawa, and H. Okamoto, Nano Lett. **11**, 960 (2011).

[29] H.A. Atwater and A. Polman, Nature Mat. **9**, 205 (2010).

[30] J.-L. Wu, F.-C. Chen, Y.-S. Hsiao, F.-C. Chien, P. Chen, C.-H. Kuo, M.H. Huang, and C.-S. Hsu, ACS Nano **5**, 959 (2011).

[31] A.G. Curto, G. Volpe, T.H. Taminiau, M.P. Kreuzer, R. Quidant, and N.F. van Hulst, Science **329**, 930 (2010).

[32] N. Livneh, A. Strauss, I. Schwarz, I. Rosenberg, A. Zimran, S. Yochelis, G. Chen, U. Banin, Y. Paltiel, and R. Rapaport, Nano Lett. **11**, 1630 (2011).

[33] P. Mühlschlegel, H.-J. Eisler, O.J.F. Martin, B. Hecht, and D.W. Pohl, Science **308**, 1607 (2005).

[34] J.N. Farahani, D.W. Pohl, H.-J. Eisler, and B. Hecht, Phys. Rev. Lett. **95**, 017402 (2005).

[35] A.W. Schell, G. Kewes, T. Hanke, A. Leitenstorfer, R. Bratschitsch, O. Benson and T. Aichele, Opt. Express **19**, 7914 (2011).

[36] I.S. Maksymov, I. Staude, A.E. Miroshnichenko, and Y.S. Kivshar, Nanophotonics **1**, 65 (2012).

[37] P. Biagioni, J.-S. Huang, and B. Hecht, Rep. Prog. Phys. **75**, 024402 (2012).

[38] R. Esteban, A.G. Borisov, P. Nordlander, and J. Aizpurua, Nature Comm. **3**, 825 (2012).

[39] X. Wu, S.K. Gray, and M. Pelton, Opt. Express **18**, 23633 (2010).

[40] A. Manjavacas, F.J. Garcia de Abajo, and P. Nordlander, Nano Lett. **11**, 2318 (2011).

[41] P. Weis, J.L. Garcia-Pomar, R. Beigang, and M. Rahm, Opt. Express **19**, 23573 (2011).

[42] S.G. Kosionis, A.F. Terzis, S.M Sadeghi, and E. Paspalakis, J. Phys.: Condens. Matter **25**, 045304 (2013).

[43] R.D. Artuso and G.W. Bryant, Phys. Rev. B **82**, 195419 (2010).

[44] R.D. Artuso and G.W. Bryant, Nano Lett. **8**, 2106 (2008).

[45] E. Waks and D. Sridharan, Phys. Rev. A **82**, 043845 (2010).

[46] A. Ridolfo, O. Di Stefano, N. Fina, R. Saija, and S. Savasta, Phys. Rev. Lett. **105**, 263601 (2010).

[47] W. Zhang, A.O. Govorov, and G.W. Bryant, Phys. Rev. Lett. **97**, 146804 (2006).

[48] S.G. Kosionis, A.F. Terzis, V. Yannopapas, and E. Paspalakis, Phys. Chem. C **116**, 23663 (2012).

[49] M. Pfeiffer, K. Lindfors, C. Wolpert, P. Atkinson, M. Benyoucef, A. Rastelli, O.G. Schmidt, H. Giessen, and M. Lippitz, Nano Lett. **10** 4555 (2010).

[50] L. Zhao, T. Ming, H. Chen *et al*, Nanoscale **3**, 3849 (2011).

[51] P. Anger, P. Bharadwaj, and L. Novotny, Phys. Rev. Lett. **96**, 113002 (2006).

[52] S.J. Barrow, X. Wei, J.S. Baldauf, A.M. Funston, and P. Mulvaney, Nature Comm. **3**, 1275 (2012).

[53] R.Y. Zhang, B. Shao, J.R. Dong, K. Huang, Y.M. Zhao, S.Z. Yu, and H. Yang, Opt. Mat. Express **2**, 173 (2012).

[54] M.C. Günendi, İrem Tanyeli, G.B. Akgŭç, A. Bek, R. Turan and O. Gülseren, to be published.

[55] The phase of the sunlight exhibit random fluctuations. This effect has second quantized origin (see Chapter 14.5 in Ref. [1] and Ref.s [57, 58]) and gives rise to a finite coherence time ($\tau \sim 10^{-8}$s) for the incident sun light. For this reason, at the end of each phase-coherence period, one shall consider a reset source. The shift in the oscillation phase of the source can interfere destructively with the previous polarization constructed on the nanometal. Thus, plasmonic and quantum oscillations are reorganized after each phase-coherence period.

[56] L.Mandel and E.Wolf, *Optical Coherence and Quantum Optics* (Cambridge University Press, Cambridge, 1995).

[57] W. Li, A.K. Tuchman, H.-C. Chien, and M.A. Kasevich, Phys. Rev. Lett. **98**, 040402 (2007).

[58] G.-B. Jo, Y. Shin, S. Will, T.A. Pasquini, M. Saba, W. Ketterle, D.E. Pritchard, M. Vengalattore, and M. Prentiss, Phys. Rev. Lett. **98**, 030407 (2007).

[59] A. Benedetti, M. Centini, C. Sibilia, and M. Bertolotti, J. Opt. Soc. Am. B **27**, 408 (2010).

[60] Such oscillators can be modelled in the classical regime using Maxwell equations [11].

[61] Near the resonance $\omega = \omega_q = \omega_{\rm eg}$, there occurs a second real root for y. The system of equations we study is nonlinear. Thus, convergence to one of the steady states depends on the initial value [62]. We check that; for the initial conditions $\rho_{\rm gg}(t=0) = 1$, $\rho_{\rm eg}(t=0) = 0$ and $q(t=0) = 0$, real-time simulations of Eq. (4-6) converges to the plotted results.

[62] Steven H. Strogatz, *Nonlinear Dynamics and Chaos* (Perseus Books Publishing L.L.C., New York, U.S.A, 1994).

[63] D. Pacifici, H. Lezec, H.A. Atwater, Nature Photon. **1**, 402 (2007).